MICROBUNCHING STUDIES FOR SPARX PHOTOINJECTOR

C. Ronsivalle, ENEA C.R. Frascati, Frascati (Roma), Italy
M. Ferrario, C.Vaccarezza, INFN/LNF, Frascati (Roma), Italy
M. Migliorati, Rome University La Sapienza, Roma, Italy
M. Venturini, LBNL, Berkeley CA, USA

Abstract

The SPARX X-FEL accelerator will be the first FEL facility to operate with a hybrid (RF plus magnetic chicane) compression scheme. Numerical studies of propagation of beam density modulations stemming from photogun laser, through the photoinjector operating under velocity bunching conditions have been carried out. A semi-analytical model for the linear gain in a RF compressor is also being developed and some preliminary results are presented.

INTRODUCTION

The use of RF compression or "velocity bunching" technique [1] to contribute (at least in part) to beam compression is appealing in many ways. The possibility to achieve RF compression without emittance degradation has been recently demonstrated for a beam charge of 200-300 pC and a 7 psec FWHM pulse in the SPARC accelerator [2], that is the prototype of the injector of the SPARX FEL facility [3] in which a hybrid (RF plus magnetic chicane) compression scheme will be employed. For this reason it is important to characterize in the SPARX phtoinjector the RF compression from the point of view of the microbunching instability, one of the possible causes of degradation of the FEL performance.

MICROBUNCHING MODELING UNDER VELOCITY BUNCHING OPERATION

Modeling of μbunching in RF compressors is more delicate than in magnetic compressors. Some simplifying assumptions may not hold or may not hold as well (e.g. longitudinal density is not 'frozen'; linear approximation of beam dynamics under external forces may be accurate only in very limited cases; 1D LSC impedance model may be not very appropriate …). So numerical and semi-analytical models have been developed and some results of this study have been used in [4], where the perfomance of the two different compression schemes, (velocity bunching plus magnetic compressor and purely magnetic) in the SPARX accelerator is compared against the microbunching instability.

Numerical Calculations

The SPARX photoinjector consists of a 1.6 cell RF gun (BNL/SLAC/UCLA type) including a Copper photocathode with an emittance compensating solenoid followed by three 3-meters long SLAC-type travelling wave sections operating at 2856 MHz with the first two accelerating sections embedded in a solenoid.

It is foreseen to operate in different configurations with high charge (1 nC) or low charge (200-50 pC) able to inject in the SPARX accelerator different beams satisfying the users requirements. The high charge working point is splitted into two operating modes depending on whether the RF compression is used or not (Table 1).

Table 1: SPARX injector high charge WP parameters.

Input parameters	Output parameters (no RF compression)	Output parameters (RF compression factor ~3.2)
Q=1 nC σ_{xy}(cathode)= 0.55 mm Flat pulse (FWHM=10 ps, rise time=1 ps)	I_{peak}=96 A ε_n=1mm-mrad σ_z=904 μm σ_E/E=0.15%	I_{peak}=309 A ε_n=1.2 mm-mrad σ_z=280 μm σ_E/E=1.04%

The response to different density modulations stemming from the photogun laser in a range of modulations wavelengths (λ_m=50-300 μm) with a ripple of ±5% has been studied by using PARMELA code with a number of particles N_p=1.5M for the SPARX high charge working point with RF compression.

In Fig. 1 the computed evolution of the current profile with a density modulation of λ_m=150 μm at the cathode is shown up to the linac output.
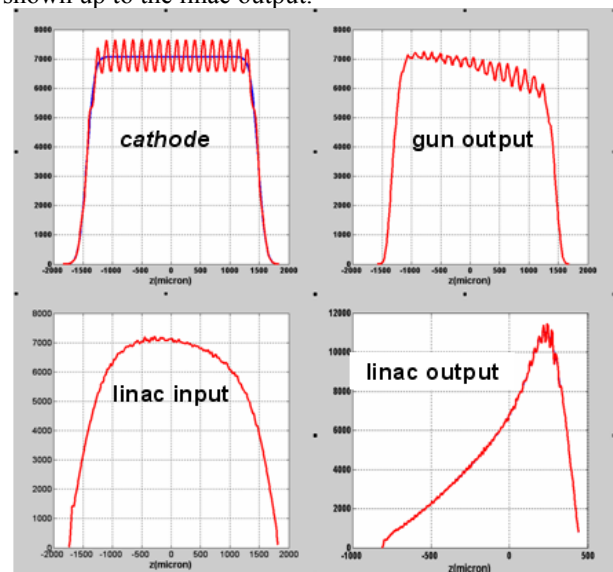
Figure 1: Evolution of current profile with a modulation of λ_m=150 μm at the cathode.

The corresponding evolution of the energy distribution is shown in Fig.2. One can see that the density modulation is completely converted in energy modulation at the linac entrance and after the bunching and the acceleration in the three TW sections the energy modulation is partially reconverted in a modest density modulation (the gain is clearly <1) and in a residual energy modulation.
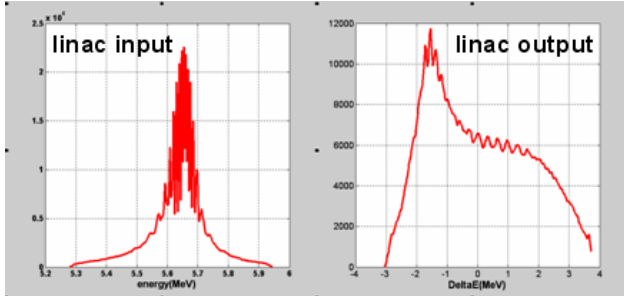
Figure 2: Energy distribution at the linac input and output with a modulation of λ_m=150 μm at the cathode.

The plot of Fig. 3 with the evolution of the amplitude of density and of the energy modulation in the drift before the TW sections show how the longitudinal space charge forces transform the initial current density modulation in energy modulation for three different initial modulations wavelengths The jump from zero to 15 cm occurs in the RF gun. As expected the amplitude of modulation energy increases with the wavelength.
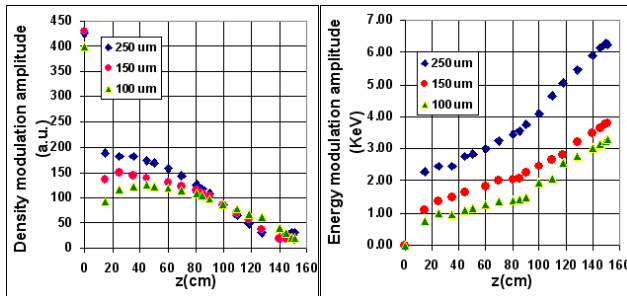
Figure 3: Evolution of density (right plot) and energy modulation (left plot) in the drift space before the linac sections.

For the computation of the amplitude and the wavelength of the dominant component of the Fourier spectrum of the modulated output beam distributions, two techniques of analysis have been used: the FFT analysis of the output beam distribution with initial modulation and the FFT analysis of the difference between the output beam distributions with and without initial modulation. The second technique acts as a noise filter and is particularly suitable for short wavelengths. Figure 4 shows the plot of the wavelength of the output density modulation versus the density modulation at the cathode retrieved by the two techniques (the second technique allows to find the point at the shortest modulation wavelength). Due to the bunch shape deformation given by the combined action of the RF non-linearity and the

space charge the output modulation wavelength is 1/5 of the initial modulation wavelength.
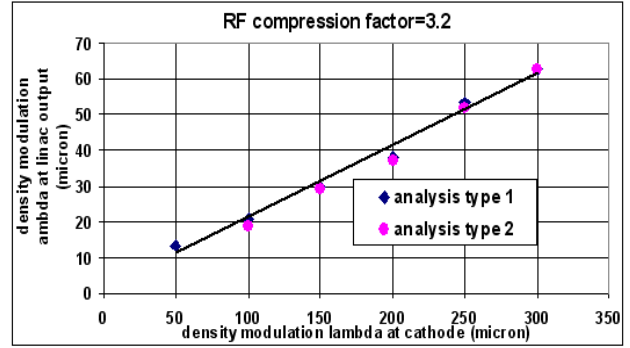
Figure 4: Output wavelength *vs* input modulation wavelength for a compression factor=3.2.

The plots of the FFT spectra retrieved by using the two techniques are reported in figure 5 for a modulation at the cathode of λ_m=150 μm.
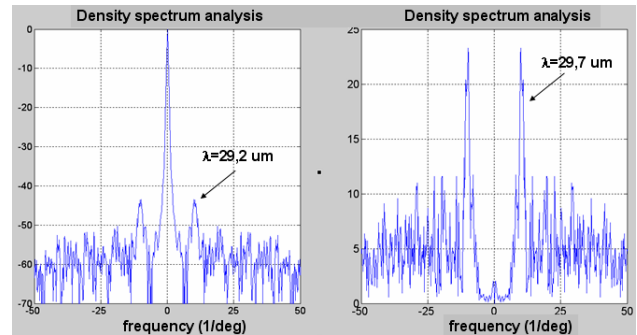
Figure 5: Initial modulation of λ_m=150 μm, FFT analysis of output beam density distribution: (left) modulated beam (right) modulated-unmodulated beam.

The output modulation density at the linac output, in all the explored range of modulations (limited by the number of particles used in simulation), is shown in the plot of figure 6.
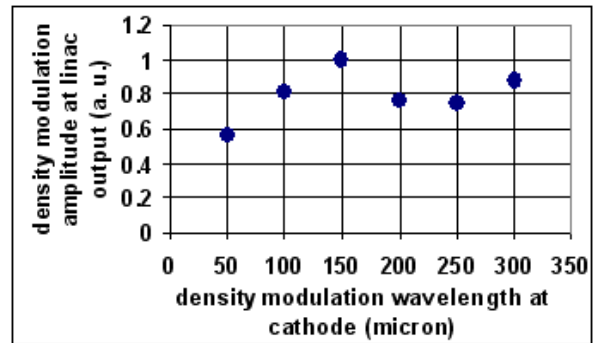
Figure 6: Density modulation amplitude *vs* modulation wavelength at cathode.

Semi-Analytical Model of the Linear Gain in a RF Compressor

In order to assist with the investigation of the various mechanisms affecting the evolution of longitudinal modulations in the RF compressor (RFC) we have started

to develop theoretical models for the first-order evolution of beam density and energy modulations in a beamline composed of a drift space followed by a single RFC. Here we report some preliminary results. Theoretical models embodying varying degrees of accuracy and complexity are conceivable (see [5] for more details). The crudest approach is an extension to RF compressors of the model used in [6] to calculate the linear gain function in magnetic compressors. In this approximation space charge is active only in the drift before the RFC, whilst no collective effects are considered in the RFC. The linear gain for a beam with Gaussian energy density is given by

$$ G = \frac{I_0}{I_A} \cdot \frac{|Z_{LSC}| \cdot S}{Z_0} \left(|M_{12}| Ck \right) \cdot \exp\left(\frac{-\left(M_{12} Ck \sigma_p \right)^2}{2} \right) \quad (1) $$

where I_0 is the uncompressed beam current, I_A is Alfven current, Z_{LSC} is the impedance due to longitudinal space charge[7] for unit length averaged on the beam radius, Z_0 is the vacuum impedance, σ_p is the uncorrelated energy spread, k is the wave number of the initial modulation, the

term $S = \dfrac{\sin(\omega_{sc} L_d / c)}{\omega_{sc} / c}$ with

$$ \frac{\omega_{sc}}{c} = \left[\frac{I_0 k}{I_A \gamma^3} \cdot |Z_{LSC}(k) / Z_0| \right]^{1/2} $$

takes into account the plasma oscillations in the drift and

$$ C = \frac{1}{M_{11} - h M_{12}} $$

is the compression factor (*h*=initial chirp) with M_{ij} being the elements of the linear transfer map obtained by linearizing the equations of motion in deviation variables $(\Delta z, \Delta \gamma)$ around the reference particle. The next level of approximation consists of extending the effect of the longitudinal space charge through the RF compressor using the same 1D model of LSC impedance as in the leading drift. This requires the numerical solution of an integral equation. Curves obtained from these two models are compared in Fig.7 for the SPARX beam parameters (96A, 5.6MeV, C=3.2, RFC length=3m, E_{acc}=23.5 MV/m).
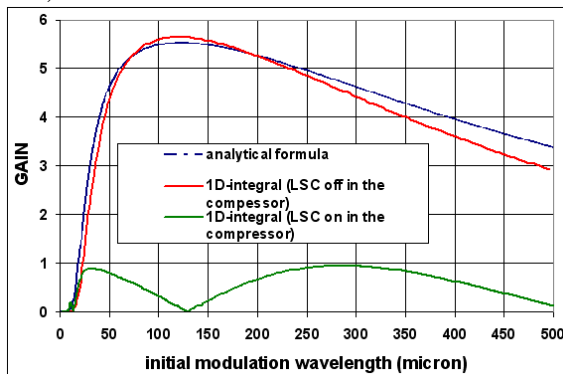
Figure 7: Linear gain at the exit of RF compressor *vs* initial modulation wavelength for a coasting beam.

In the model the drift length and the beam radius (L_d=0.5 m, r_b=0.84 mm) have been chosen in order to maximize the conversion of the initial density modulation in energy modulation at the entrance of the compressor. One can see that the analytical formula and the numerical solution with the LSC off in the RFC are in good agreement, but when the longitudinal space charge is switched on in the RF compressor the gain is strongly damped because of the space-charge induced oscillations. The sensitivity of the gain to the magnitude of the uncorrelated energy spread, which tends to smear the microbunching at lower wavelengths, is shown in Fig. 8.
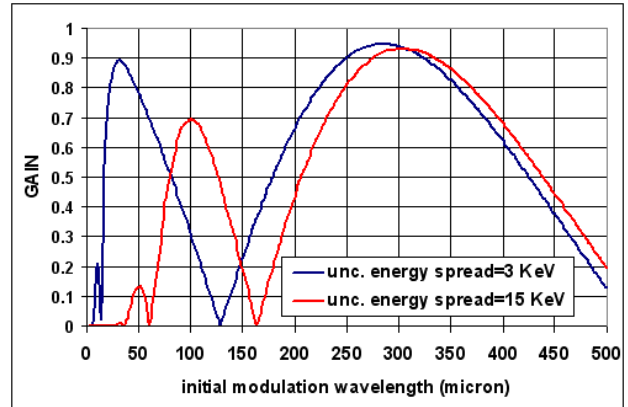
Figure 8: Linear gain for two different values of the uncorrelated energy spread for a coasting beam.

The model described here may be useful to determine some basic scaling but has still some obvious limitations (infinitely long beam, linear chirp, constant radius of the beam transverse density throughout drift and RFC, etc.). An investigation of its actual relevance and comparisons against macroparticle simulations are still on-going and will be documented in [5]. A possible improvement consists in an extension of the theory to encompass the case of a Gaussian longitudinal density, at the cost of increasing the dimensionality of the integral equation for the linear gain. Further refinements should also include an account of the radial dependence of the longitudinal component of the electric field induced by space charge.

REFERENCES

[1] L. Serafini and M. Ferrario "Velocity bunching in photoinjectors", AIP Conference Proceedings.

[2] M. Ferrario et al., "Velocity Bunching Experiments at SPARC", these Proceedings.

[3] L. Palumbo et al., "Status of SPARX Project", Proceedings of EPAC08, Genoa, Italy, p. 121.

[4] C. Vaccarezza et al., "Microbunching Instability Modeling in the SPARX Configurations", these Proceedings.

[5] M. Venturini, M. Migliorati, C. Ronsivalle, and C. Vaccarezza, "Linear Gain for the Microbunching Instability in an RF compressor", in preparation.

[6] E.L. Saldin et al., NIM A483 (2002) p.516.

[7] Z. Huang and T. Shaftan, SLAC-PUB-9788 (August 2003).